Proceedings of the ASME 2022
Internal Combustion Engine Division Fall Technical Conference
ICEF2022
October 16-19, 2022, Indianapolis, Indiana

ICEF2022-90257

DESIGN OPTIMIZATION OF AN ETHANOL HEAVY-DUTY ENGINE USING DESIGN OF EXPERIMENTS AND BAYESIAN OPTIMIZATION

Bulut Tekgül
Argonne National Laboratory, Lemont, IL
Email: btekgul@anl.gov

I-Han Liu
Argonne National Laboratory, Lemont, IL

Manohar Vittal
ClearFlame Engines, Chicago, IL

Robert Schanz
ClearFlame Engines, Chicago, IL

Bernard H. Johnson
ClearFlame Engines, Chicago, IL

Julie Blumreiter
ClearFlame Engines, Chicago, IL

Gina M. Magnotti
Argonne National Laboratory, Lemont, IL

ABSTRACT

Diesel-fueled engines still hold a large market share in the medium and heavy-duty transportation sector. However, the increase in fossil fuel prices and the strict emission regulations are leading engine manufacturers to seek cleaner alternatives without a compromise in performance. Alcohol-based fuels, such as ethanol, offer a promising alternative to diesel fuel in meeting regulatory demands. Ethanol provides cleaner combustion and lower levels of soot due to its chemical properties, in particular its lower level of carbon content. In addition, the stoichiometric operating conditions of alcohol fueled engines enable the mitigation of NOx emissions in aftertreatment stage. With the promise of retrofitting diesel engines to run on ethanol to reduce emissions, the thermal efficiency of these engines remains the primary optimization target. In order to find the optimal ethanol-fueled engine design that maximizes the thermal efficiency, a large design space needs to be investigated using engineering tools.

In this study, previous research by the authors on optimizing the design of a single-cylinder ethanol-fueled engine was extended to explore the design space for a heavy-duty multi-cylinder engine configuration. A heavy-duty engine setup with multiple operating conditions at different engine speeds and loads were considered. A design optimization analysis was performed to identify the potential designs that maximize the indicated thermal efficiency in an ethanol-fueled compression ignition engine. First, a computational fluid dynamics (CFD) model of the engine was validated using experimental data for four drive cycle points. Using a design of experiments (DoE) approach and a parameterized piston bowl geometry, the model was then exercised to explore the relationship among geometric features of the piston bowl and spray targeting angle and indicated thermal efficiency across all tested operating conditions. After evaluating 165 candidate designs, a piston bowl geometry was identified that yielded an increase between 1.3 to 2.2 percentage points in indicated thermal efficiency for all tested conditions, while satisfying the operational design constraints for peak pressure and maximum pressure rise rate. The increased performance was attributed to enhanced mixing that led to the forma-

tion of a more homogeneous distribution of in-cylinder temperature and equivalence ratio, higher combustion temperatures, and shorter combustion duration. Finally, a Bayesian optimization (BOpt) analysis was employed to find the optimal piston bowl geometry with a fixed spray injector angle for one of the operating conditions. Using BOpt, a piston candidate was identified that resulted in a 1.9 percentage point increase in thermal efficiency from the baseline design, yet only required 65% of the design samples investigated using the DoE approach.

1 INTRODUCTION

Diesel-fueled compression-ignition (CI) engines are still heavily used in heavy-duty applications, especially in the hard-to-electrify sectors such as marine, rail and on-highway transportation [1]. In particular, diesel-fueled CI engines offer high performance and low maintenance due to their high efficiency, high power density, and relatively simplistic design. However, stringent soot and NOx emission requirements are leading engine manufacturers to explore decarbonization strategies and alternatives to diesel fuel.

Alcohol fuels, such as methanol and ethanol, offer a promising alternative to diesel fuel in meeting regulatory emission demands. Due to their low soot propensity properties, utilizing alcohol fuels can significantly lower soot emissions [2]. In addition, lowering soot emissions may simplify the exhaust aftertreatment of NOx emissions through three-way catalysis (TWC), a method otherwise unavailable due to the prohibitively high levels of soot at the stoichiometric air-fuel ratio (AFR) conditions in diesel-fueled CI engines [3]. These factors make alcohol-fueled CI engines a promising alternative, with comparable performance and efficiency to diesel-fueled engines. However, a set of modifications need to be undertaken to allow the usage of alcohol fuels in CI engine configurations.

Historically, alcohol fuels have not been used in CI engines due to their low cetane number and high auto-ignition temperatures [4]. In order to ignite these fuels within a reasonable time window under compression, higher in-cylinder temperatures are needed at the time of injection [5]. One method to elevate the in-cylinder temperature in CI engines is through the application of thermal barrier coatings (TBCs) on selected surfaces to reduce the heat loss from the boundaries [6–8]. While this application may cause overheated charge and tendency to knock in conventional spark ignition (SI) engines, TBCs can enable reliable autoignition of alcohol fuels in CI engines [8]. With the mitigation of ignition and emissions concerns through the use of alcohol fuels, TBCs, and TWC aftertreatment, the performance metrics of such a system can be focused on thermal efficiency. In order to achieve comparable or superior thermal efficiency relative to a diesel CI engine, an optimization study is needed to explore the design trade-offs between piston bowl geometries and spray targeting strategies.

While a design optimization analysis of alcohol-fueled CI engines is needed to unlock their true potential, experimental testing with hardware iterations is costly and limits the design space that can be explored effectively. 3-D computational fluid dynamics (CFD) simulations are a complementary tool in the design exploration process. Recently, a number of studies utilized CFD for design optimization process of different engineering problems. Pei et al. performed a geometry and combustion recipe optimization of a heavy-duty CI engine using a DoE approach with 3-D CFD simulations [9]. Moiz et al. utilized a machine learning genetic algorithm (ML-GA) approach to optimize the combustion recipe of a Cummins ISX15 CI engine [10]. More recently, Owoyele et al. performed simulation-driven design optimization of CI engine operating conditions (e.g., intake temperature, injection timing) to optimize soot, NOx and pressure rise rate levels. In their work, different machine learning based approaches were coupled with the CFD simulations to explore and identify promising regions of the design space [11,12]. Following their efforts, Badra et al. used a similar approach for optimizing light and heavy-duty gasoline CI engine designs [13]. Magnotti et al. employed a DoE approach for optimizing an ethanol fueled engine, laying the groundwork for this study [7]. In summary, coupling CFD simulations with design optimization strategies is an effective way to perform engine design optimization for a given design space and an optimization target.

In this study, 3-D CFD simulations coupled with two different design optimization methods were employed to investigate the piston bowl geometry-injector angle design space and find candidate designs that maximize the indicated thermal efficiency of an ethanol-fueled CI engine. A sector mesh 3-D CFD model with 1-D conjugate heat transfer (CHT) boundary conditions was employed to model a CI engine with TBCs applied to its head and piston bowl boundaries. The model framework was validated against experimental data at four different engine operating conditions. After the parameterization of the piston bowl geometry, DoE and Bayesian optimization (BOpt) methods were used to find candidate piston bowl-injector angle configurations that maximize the indicated thermal efficiency. A more in-depth analysis was performed to find underlying design rules and combustion characteristics that result in thermal efficiency improvements.

The present study is organized as follows: First, the experimental setup and operating conditions used for CFD model validation is introduced and described in Section 2. Then, details on the numerical setup including the CFD framework and utilized design optimization methods are described in Sections 3 and 4. Results obtained from the numerical analysis are presented in Section 5. Finally, Section 6 provides an overall summary of the findings and the conclusion.

2 EXPERIMENTAL SETUP

The focus of this study is the characterization and optimization of a 6-cylinder Cummins X15 engine that has been converted to run on ethanol fuel. A schematic of the engine setup is presented in Figure 1. Details on the engine and fuel injector, as well as investigated operating conditions, are provided in Tables 1 and 2.

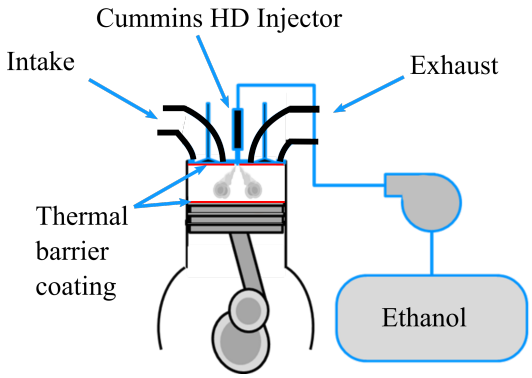

FIGURE 1: SCHEMATIC OF THE CUMMINS X15 ENGINE AND ITS INJECTION SYSTEM, WITH THERMAL BARRIER COATING.

To establish and validate a CFD model that can be utilized in a design optimization study to maximize thermal efficiency, four different operating conditions over a range of loads and engine speeds were selected for the experimental analysis, as summarized in Table 2. One of these operating points was also compared to a diesel-fueled simulation and experimental data at the same speed and load, to enable a comparison between diesel and ethanol fueled engine performance. For ethanol-fueled conditions, a thin layer of TBCs material was applied on the cylinder head and piston bowl to reduce the heat loss, and promote the ignition of the injected ethanol by increasing the in-cylinder temperatures. All configurations feature a Cummins heavy-duty injector with a spray targeting angle of 75°with respect to the vertical axis.

The engine is fitted with an AVL GH15DK cylinder pressure sensor to record the in-cylinder pressure every 0.25 CAD using a high-speed data acquisition recorder and averaged over 100 engine cycles. Over the four different operating conditions, the coefficient of variance (COV) of the peak cylinder pressure was observed to be less than 0.9%, indicating consistent and reliable combustion performance and minimal cycle-to-cycle variation (CCV).

TABLE 1: ENGINE AND INJECTOR SPECIFICATIONS FOR THE EXPERIMENTAL STUDY.

Displacement [L]	14.9
Compression Ratio [-]	19.2:1
Bore / Stroke [mm]	137 x 169
Swirl Ratio [-]	0.8
Injector Type	Cummins HD
Number of orifices	8
Orifice diameter [mm]	0.28
Injector angle [deg]	75
Valve Timing [CAD aTDC]	-142.5 / 145.3

3 NUMERICAL SETUP

All the engine CFD simulations in this study were performed with CONVERGE v3.0 [14], a commercial software for CFD simulations. The gas phase flow was solved by the compressible Navier-Stokes equations, consisting of conservation equations for mass, momentum, species mass fraction and enthalpy equations. A single-species diffusion model was assumed and the system of equations was closed using the Redlich-Kwong equation of state.

The finite-volume method was used to solve the governing equations using a Pressure-Implicit with Splitting of Operators (PISO) algorithm and second order spatial central differencing discretization. The gas-phase flow turbulence was modeled with the RNG k-ε turbulence model, and a standard wall function was used to handle the near-wall treatment. A dynamic refinement method was adopted at the wall boundaries to restrict the y^+ values between 30 and 100 during the combustion process. A computational mesh with a base grid size of $\Delta_x = 2$ mm and three level of fixed refinement near the injectors ($\Delta_x = 0.25$ mm) was used. The evolution of the injected fuel spray was further tracked in the combustion chamber using Adaptive Mesh Refinement (AMR) with two level of refinement based on 2^{nd} derivative of velocity and temperature ($\Delta_x = 0.5$ mm), resulting in a peak cell count around 1 million cells.

To achieve a balance between computational accuracy and expense of the simulations, a closed cycle simulation setup with a 90° sector mesh with two of the eight spray injectors from the experimental configuration was utilized, as shown in Figure 2. The closed cycle simulations began at intake valve closing (IVC) and were simulated until exhaust valve opening (EVO). The IVC thermophysical conditions (chemical composition, pressure, and temperature) were obtained by simulating a full-geometry open-cycle simulation validated by the experimental setup, and using the in-cylinder conditions at IVC of this simulation to initialize the closed-cycle simulation. This CFD setup was simulated and

TABLE 2: THERMODYNAMIC AND INJECTION CONDITIONS FOR THE FOUR OPERATING CONDITIONS INVESTIGATED IN THIS STUDY.

Case	C100 diesel	C100	C75	A100	A50
Crank speed [rpm]	1600	1600	1600	1148	1148
Brake torque [Nm]	2277	2277	1708	2508	1254
Injected fuel	Diesel*	Ethanol	Ethanol	Ethanol	Ethanol
Injector type	Cummins HD	Cummins HD	Cummins HD	Cummins HD	Cummins HD
Fuel temperature [K]	312.8	298.7	304.21	296.93	300.54
Total injected fuel mass [mg]	257.68	435.125	318.626	465.98	227.929
SOI$_{pilot}$ [CAD aTDC]	N/A	-9.538	-15.89	-5.7948	-6.96576
Injection duration$_{pilot}$ [CAD]	N/A	3.559	3.46	3.03	2.686
SOI$_{main}$ [CAD aTDC]	-5.214	-3.395	-5.51	-0.5599	-1.79976
Injection duration$_{main}$ [CAD]	23.8	30.297	23.85	28.17	14.602
Fuel rail pressure [MPa]	248.66	170.04	160.0	139.99	139.93
Intake air temperature [K]	336.76	377.37	381.82	396.43	374.43
Global equivalence ratio [-]	0.765	0.803	0.769	0.811	0.839

*Tetradecane and *n*-heptane were used as the physical and chemical surrogates of diesel fuel.

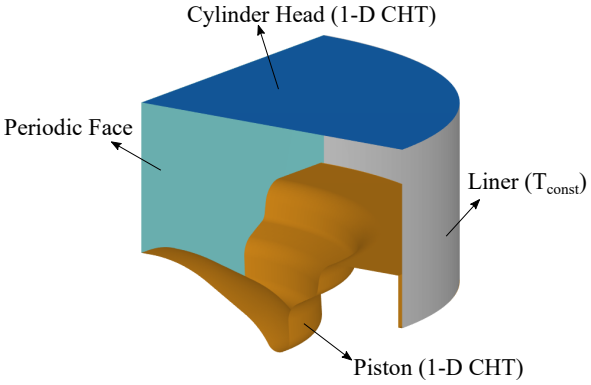

FIGURE 2: A SCHEMATIC OF THE 90° SECTOR GEOMETRY USED TO MODEL THE ENGINE WITH PRESCRIBED BOUNDARIES. NOTE THAT THE C100 DIESEL CASE DOES NOT FEATURE 1-D CHT BOUNDARY CONDITIONS.

the results were compared with the experimental data for further validation, as presented in Section 5.1.

Direct-injection of the fuel and spray development was modeled using a Lagrangian-Eulerian framework. The liquid fuel was represented as Lagrangian parcels that interact with the gas-phase Eulerian domain. The injection of the liquid spray was performed using the "blob" injection model [15], while primary and the secondary atomization of the liquid parcels were modeled using the Kelvin-Helmholtz Rayleigh-Taylor spray breakup model [16]. Droplet collisions were modeled using the No Time Counter (NTC) model [17]. Frossling correlation was used to model the evaporation between the liquid and gas phases [18]. Finally, boundary conditions for fuel-injection mass, duration and velocity were defined based on the experimentally measured rate of injection (ROI) profiles.

For ethanol-fueled cases, the injected fuel was represented as pure ethanol. A finite-rate chemistry approach was used to model the combustion process of the ethanol, by using a 80 species and 349 reaction chemical mechanism developed by Wang et al. [19]. For the diesel-fueled case, the physical properties of tetradecane was used as a diesel surrogate for liquid properties. N-heptane was used as a surrogate for gas and chemical properties, via a 42 species 168 reactions mechanism developed by Chalmers University. The chemistry computation process was accelerated by using an adaptive-zone model with temperature and equivalence ratio bin sizes of 5 K and 0.05, respectively.

Finally, to accurately model the heat transfer through the cylinder head and piston surfaces during combustion in the presence of TBCs (i.e., ethanol-fueled cases), a 1-D conjugate heat transfer (CHT) boundary condition was utilized for cylinder head and piston boundaries. This approach enables the modeling of the metal engine surfaces and the thinly applied TBCs, providing more accurate prediction of the surface temperatures by taking the heat convection between the fluid and solid phases, and conduction within the solid region in piston and head boundaries. Table 3 shows the bulk temperature boundary condition was assigned to piston and head boundaries for each condition to provide good agreement with the experimental results. Further details on the application of this model to the engine numerical modeling framework can be found in [7].

TABLE 3: BULK TEMPERATURE BOUNDARY CONDITIONS FOR THE 1-D CHT MODEL FOR ALL ETHANOL-FUELED OPERATING CONDITIONS.

Case	C100	C75	A100	A50
Head Bulk Temperature [K]	458	428	428	410
Piston Bulk Temperature [K]	458	428	428	410

4 DESIGN OPTIMIZATION

This section provides a detailed description of the two design optimization methods, namely design of experiments (DoE) and Bayesian optimization (BOpt), utilized in this study. DoE approach is based on sampling design candidates in a multi-dimensional design space in a structured manner to investigate the relationship between the design parameters (input) and the response (output, merit value). BOpt approach is a sequential strategy for adaptively sampling the design space to maximize the merit value while using less samples relative to the DoE method. Further information on both these approaches are given in this section.

4.1 Design of Experiments

To explore a multi-dimensional design space for identifying an optimal design, sufficient candidates in the design space are sampled to evaluate their response (i.e., merit value). One of the most widely used multi-parameter optimization methods is the DoE approach [20]. This approach is based on sampling design candidates in a multi-dimensional design space in a structured manner to investigate the relationship between the design parameters (input) and the response (output). In this study, a DoE approach was used to identify design candidates that improve the thermal efficiency of the ethanol-fueled engine in the piston bowl geometry-spray targeting angle design space. First, the design geometry was parameterized using 11 independent design features, as shown in Figure 3. "Lip Radius" and the "Spray Angle" were defined as dependent input features. Lip Radius was adjusted separately for any given optimized design in order to create a geometry with the same compression ratio (CR = 19.2:1) of the baseline experimental condition. In addition, the spray targeting angle was automatically set to target the rim of the piston bowl for all the designs candidates.

A commercial software for automated design analysis called CAESES [21] was used to generate candidate designs for different piston bowl geometry and spray targeting angle configurations. Using CAESES, candidate designs were created based on the parameterized geometry described in Figure 3. Ranges were defined for each design feature characterizing the parameterized geometry. Using Latin Hypercube Sampling method [22], a total of 165 candidate designs were sampled. Finally, the piston geometries along with all the necessary input files for the CON-

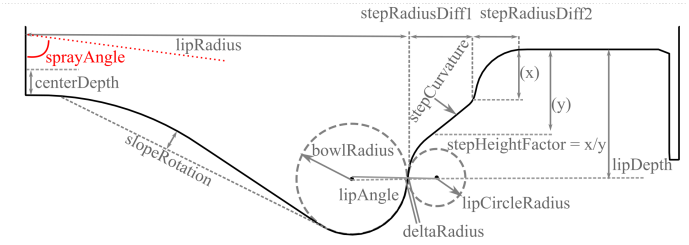

FIGURE 3: PARAMETERIZED PISTON BOWL GEOMETRY PROFILE WITH DESIGN PARAMETERS. SPRAY ANGLE (SHOWN IN COLOR) IS A DEPENDENT DESIGN PARAMETER BASED ON THE OTHER DESIGN FEATURES.

VERGE CFD simulations were generated using CAESES. The 165 unique piston designs that are considered in this study are illustrated in Figure 4 along with the baseline piston design.

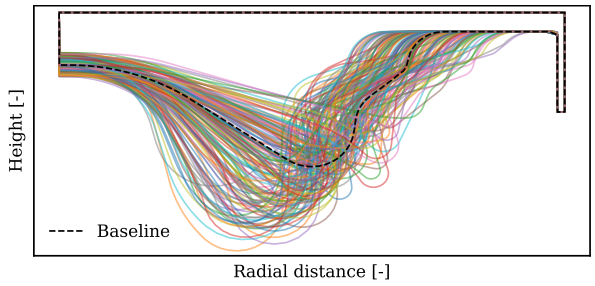

FIGURE 4: DIFFERENT NORMALIZED PISTON GEOMETRIES GENERATED WITH DOE ALONG WITH THE BASELINE PISTON GEOMETRY.

4.2 Bayesian Optimization

While DoE method defines sample points in the design space, in some cases it may require a large number of samples to properly sample a multi-dimensional design space, and produce an accurate response surface model [23]. In contrast to DoE which relies on an a priori sampling strategy, BOpt is an active learning based approach that iteratively samples the design space to maximize the value of a given merit function [24]. BOpt method employs gaussian processes (GP) to represent an unknown function that maps inputs (i.e., investigated design parameters) to an output (i.e., target merit value). While a brief description of GP modeling approach was presented here, more detailed discussion on GP's can be found in Mondal et al. [25] and Rasmussen and Williams [26].

GP approach assumes a jointly Gaussian probability distribution for any finite output collection to be modeled. In this study, GP's are used to form a surrogate model on the existing

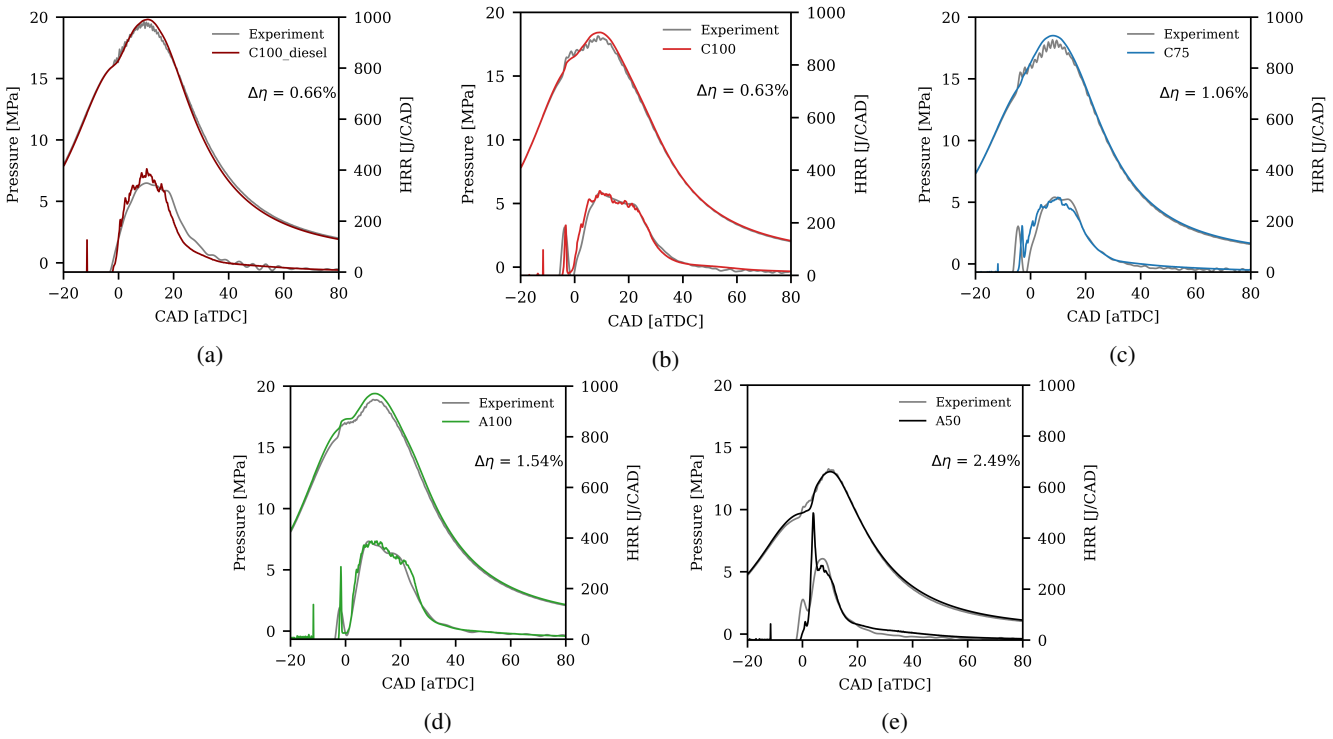

FIGURE 5: VALIDATION OF THE ENGINE SECTOR CFD MODEL AGAINST THE EXPERIMENTAL DATA FOR ALL OPERATING CONDITIONS. THE DIFFERENCE IN EXPERIMENTAL AND CALCULATED THERMAL EFFICIENCY, $\Delta\eta$, IS INDICATED FOR EACH CONDITION.

dataset using a kernel function f. The BOpt approach uses the GP surrogate model to sample new design candidates that maximize the merit function value [27]. BOpt models can be employed to explore the regions of the design space with no or little sampled points (exploration), or focus on regions already maximizes the target merit value to find more optimal design samples (exploitation). Balancing exploration and exploitation in the sampling strategy provides a path to optimally sample a multi-dimensional design space with less samples than traditional DoE-based approaches.

In this study, the GPyOpt package developed by University of Sheffield was used for performing a BOpt analysis [28]. First, the performance of different acquisition functions were investigated on a test problem [29] to pick the ideal acquisition function and exploration weight in exploring the multi-dimensional design space for new candidate designs. Then, the baseline design was used as an initial condition to find a piston bowl geometry that maximizes the thermal efficiency with a fixed spray targeting angle.

5 RESULTS

5.1 Model Validation

The engine modeling setup presented in Section 3 was validated by comparing the numerical results against the engine experiments at four different operating conditions (and the diesel-fueled condition). The measured and predicted pressure and apparent heat release rate (AHRR) profiles were compared to ensure that the CFD model can accurately represent all the operating conditions and it is able to capture the changes in operating conditions described in Table 2.

A comparison of the simulated and experimental pressure traces of the operating conditions presented in Table 2 is given in Figure 5. Overall, the model was able to accurately capture the response of the in-cylinder pressure trace and apparent heat release rate (AHRR) to changes in engine speed and load. A good agreement can be observed across all tested operating conditions with a maximum deviation of peak pressure about 0.1 MPa across all conditions. Although the CFD model predicts higher early heat release rate (HRR) associated with the first injection for the lower engine speed cases (A100 and A50), the simulations were able to accurately capture the overall trend in pressure trace, as well as the HRR, and indicated thermal efficiency. The level of agreement between the measured and predicted thermal

efficiency, $\Delta\eta$ was less than 2.5 percentage points across all conditions.

5.2 Piston Bowl and Injector Angle Design Optimization

Using the 165 candidate designs generated with CAESES, a total of 660 3-D engine CFD simulations were performed for the four ethanol-fueled operating conditions (C100, C75, A100 and A50). For the optimization study, the merit function was defined as a function of the indicated thermal efficiency η_i at each operating condition, defined as:

$$\eta_i = \frac{\int_{V_{IVC}}^{V_{EVO}} pdV}{m_f \times LHV} \tag{1}$$

where subscript i is the operating condition (i.e., C100, C75, A100 and A50), m_f is the injected fuel mass, and LHV is the lower heating value of the injected fuel. For the optimization study, the merit function was defined as η_w, the weighted average of the thermal efficiencies η_i calculated across four operating conditions for each design candidate, as defined in Equation 2. A larger weight of 40 % was assigned to A50 condition due to its prevalence in the drive cycle of interest. Two design constraints for maximum peak pressure (P_{max}) and maximum pressure rise rate (PRR_{max}) with respect to baseline conditions were also imposed to filter out designs that do not satisfy the mechanical design constraints. Restricting PRR in the design optimization process is important to avoid combustion noise and possible engine damage. For reference, at baseline conditions investigated the PRR ranges between 0.7 to 1.1 MPa/CAD between the four operating conditions.

$$\eta_w = \begin{cases} 0.4\times\eta_{A50} + 0.2\times\eta_{A100} + , & \text{if } (\forall P_{max} \leq 1.05\times P_{maxbase}) \wedge \\ 0.2\times\eta_{C100} + 0.2\times\eta_{C75} & (\forall PRR_{max} \leq 2.0\text{MPa/CAD}) \\ 0, & \text{otherwise.} \end{cases} \tag{2}$$

A comparison of the weighted thermal efficiencies across the design space with respect to the baseline design is presented in Figure 6. In the sampled design space, candidate designs result in a distribution of weighted thermal efficiency performance relative to the baseline design. Design 125 is highlighted in Figure 6, hereafter named "Best Design", due its performance in maximizing the weighted thermal efficiency across all four operating points, while satisfying the maximum pressure and pressure rise rate requirements. The piston bowl profiles of the baseline and best designs are compared in Figure 7. It can be observed that the Best Design has a piston bowl rim closer to the centerline (i.e., a lower Lip Radius), as well as a deeper spray targeting angle compared to the baseline design.

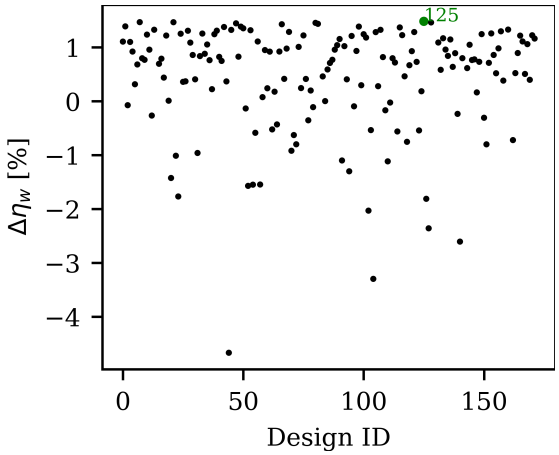

FIGURE 6: CHANGE IN WEIGHTED THERMAL EFFICIENCY OF THE DOE DATASET WITH RESPECT TO THE BASELINE DESIGN, $\Delta\eta_W$, ACROSS FOUR OPERATING CONDITIONS.

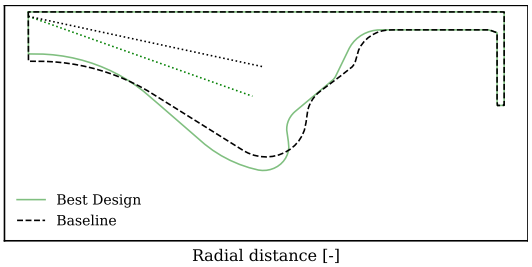

FIGURE 7: BEST DESIGN AND ITS CORRESPONDING SPRAY TARGETING ANGLE SELECTED FROM THE DOE BASED ON THE MERIT FUNCTION DEFINITION.

After the selection of the best design based on the criteria defined in Equation 2, further analysis was performed to understand the underlying mixing and combustion differences that lead to higher thermal efficiency. First, the increase in thermal efficiency across the four operating conditions was calculated, as presented in Figure 8. In this Figure, $\Delta\eta$ was defined as the relative improvement in efficiency with respect to the ethanol-fueled baseline designs, as described in Table 2. First, the C100 condition was evaluated to understand the performance differences between diesel and ethanol fuels at the same operating point and

piston bowl design. It was observed that the diesel-fueled setup shows an increase in efficiency around 2 percentage points with respect to the ethanol-fueled baseline design. A comparison of the thermal efficiency performance of the ethanol-fueled Best Design against the baseline design revealed 1.3 to 2.2 percentage points increase across all four operating conditions. This analysis confirms the hypothesis that it is possible to achieve comparable efficiency as the diesel baseline when the piston bowl and spray targeting angle is allowed to be optimized for ethanol fuel use at stoichiometric conditions.

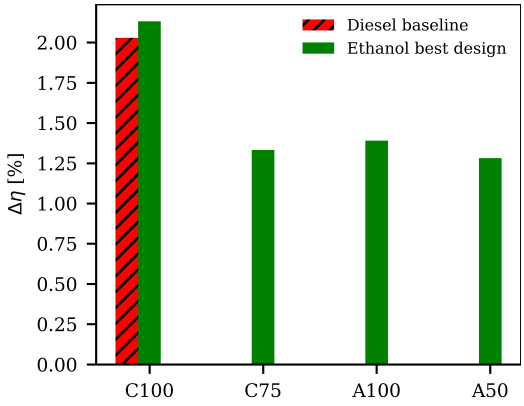

FIGURE 8: CHANGE IN THERMAL EFFICIENCY ACROSS FOUR OPERATING CONDITIONS WITH RESPECT TO ETHANOL BASELINE DESIGN. DIESEL CASE IS ALSO PRESENTED FOR C100 OPERATING CONDITION.

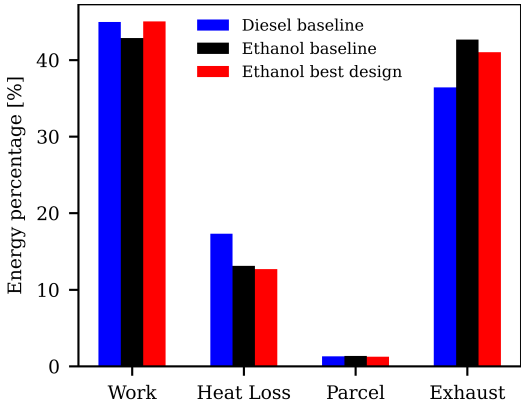

FIGURE 9: ENERGY BUDGET ANALYSIS OF THE C100 CASE FOR DIESEL, ETHANOL BASELINE, AND ETHANOL BEST DESIGN CONDITIONS.

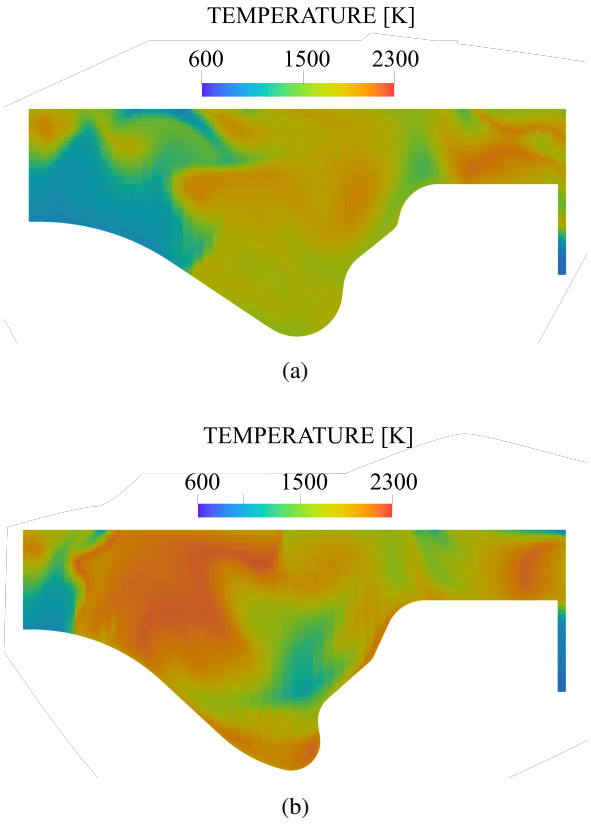

FIGURE 10: IN-CYLINDER TEMPERATURE DISTRIBUTION OF (a) BASELINE AND (b) BEST DESIGN AT 20 CAD ATDC FOR A50 CONDITION.

To gain a better understanding of the factors driving the efficiency improvement for the best design, an energy budget analysis was performed for the C100 operating condition and presented in Figure 9. C100 condition was chosen due to the existence of diesel-fueled experimental data at this operating condition. The energy converted to useful work, heat loss through the boundaries, liquid parcel heating and evaporation, and increasing the internal energy of the final gas mixture (exhaust) was calculated between IVC and EVO, and divided by the total energy potential introduced to the system:

$$Q_f = m_f \times LHV, \tag{3}$$

where Q_f is the total energy potential in the system due to injected fuel. The LHV value was selected to be 27.7 MJ/kg for ethanol and 43.5 MJ/kg for diesel. It can be observed that the percentage of heat loss is higher for the diesel case due to lack of TBCs material applied on the boundaries. This increased heat loss also presents itself as lower exhaust energy as opposed to ethanol-fueled conditions. Comparable energy for parcel heat-

ing was noted across all three conditions. Finally, it can be observed that the ethanol best design demonstrates a higher work percentage than ethanol baseline, and comparable with the diesel baseline condition.

The impact of the new piston bowl geometry on in-cylinder mixing and combustion was investigated to explore its relationship with the increase in thermal efficiency. Figure 10 shows a comparison of the temperature distributions at 20 CAD aTDC for the (a) baseline and (b) best designs at the A50 condition. At the time instant shown, it can be seen that the best design produces a more uniform temperature distribution relative to the baseline design, with higher peak temperatures in the central portion of the piston bowl. These results suggest that the design changes result in enhanced mixing of fuel and in-cylinder charge. In addition, for all four operating conditions higher mean temperatures were observed at the peak of the combustion process, which promotes higher reaction rates in the combustion chamber, increasing the indicated thermal efficiency. Although the higher in-cylinder temperatures lead to higher NOx production of about 10 to 12% in the best design compared to baseline, the stoichiometric air-fuel ratio of the investigated operating conditions enable the mitigation NOx emissions through a TWC aftertreatment process.

To investigate the relationship between mixing and thermal efficiency, in-cylinder distributions of equivalence ratio and temperature at key time instances during combustion were investigated. Figure 11 shows the probability density function (PDF) distribution of equivalence ratio and temperature for the same condition (A50) at 10 and 30 CAD aTDC to represent the peak and late stages of combustion. During peak combustion (10 CAD aTDC), it can be observed that the best design produces a most probable equivalence ratio of approximately 1.25 and temperature of 1900 K. During later stage of combustion (30 CAD aTDC), it can be seen that for the best design both equivalence ratio and temperature has higher PDF peak values below stoichiometry ($\phi \approx 0.85$) and at lower temperatures, respectively. This indicates enhanced mixing with less stratification, which leads to more complete combustion and increased thermal efficiency.

The analysis performed in this section identifies differences between the baseline and best designs that lead to a higher η_w across all operating conditions. Based on the observations, it is possible to achieve comparable or superior efficiency to diesel-fueled CI engines using ethanol if the piston bowl geometry and spray targeting angle are optimized. The differences in the piston bowl design and spray targeting from the best design led to improved in-cylinder mixture and temperature distribution, lower heat loss through the exhaust, and higher thermal efficiency. It was observed that enhanced in-cylinder mixing leads to less thermal stratification, and overall higher thermal efficiency across all operating conditions.

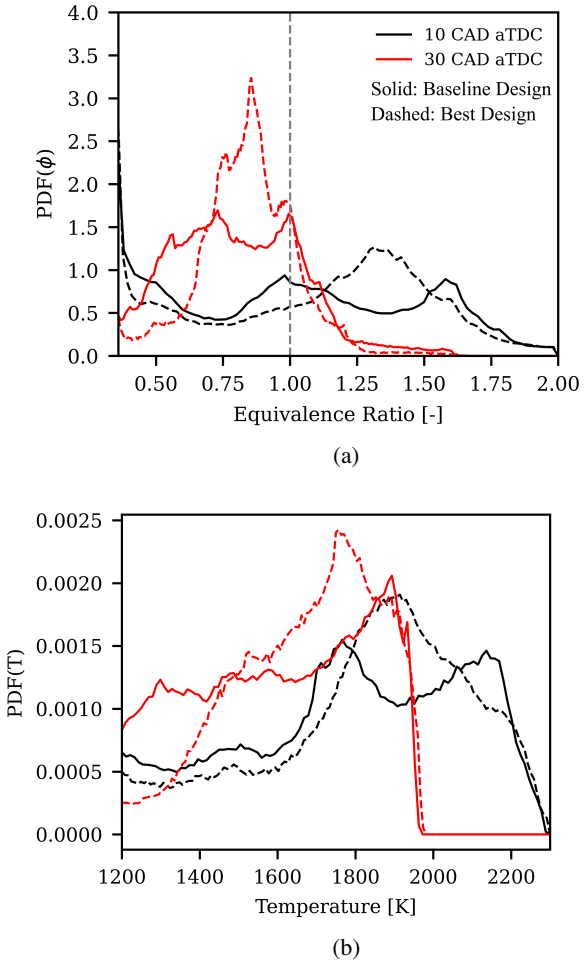

FIGURE 11: PDF DISTRIBUTION OF (a) EQUIVALENCE RATIO AND (b) TEMPERATURE AT 10 AND 30 CAD ATDC FOR A50 OPERATING CONDITION. SOLID AND DASHED LINES REPRESENT BASELINE AND BEST DESIGN, RESPECTIVELY.

5.3 Bayesian Optimization of Piston Bowl for Fixed Injector Angle

The DoE analysis performed in the previous section features the spray targeting angle as a dependent parameter that is varied to ensure spray targeting of the piston bowl rim. Such design changes would require the manufacturing of a new fuel injector tip to adjust the spray targeting location. To identify candidate designs with similar thermal efficiency gains while using the existing injector hardware, a new design optimization study was needed for the C100 operating condition where the spray targeting angle has been set as a fixed design feature.

The dataset of 165 designs across the 11-D input space was used to predict an optimal piston bowl geometry for a fixed injector angle (75°). A Gaussian Process model employing a Matern

5/2 kernel function was used to construct a response surface that forms a surrogate model over the 11-dimensional DoE dataset with varying spray targeting angle. Then, a large number of design candidates ($n = 3e5$) were sampled in a 10-dimensional (fixed spray angle) input space to predict the merit function value via the surrogate model. The design candidate with the largest predicted merit value was selected and a CFD simulation was performed to calculate the true merit value. For basis of comparison, an additional DoE analysis was performed where 165 samples were selected and simulated within the 10-D design space, where the spray targeting angle was kept as a fixed design feature. It can be observed in Figure 12 that while the prediction based on the 11-D DoE showed an improvement around 1.45 percentage points from the baseline condition (blue dotted line), the improvement obtained with a fixed spray angle 10-D DoE (gray dashed line) was much higher (around 1.88 percentage points) due to the increase in the sampling density. However, achieving this 1.88 percentage points improvement in thermal efficiency requires a new DoE analysis with fixed spray targeting angle, which is computationally expensive.

BOpt was explored as a means to identify piston bowl designs with comparable or superior performance with potentially reduced number of design samples and computational expense. First, a test problem named "six-hump camel" [29] was used to investigate the selection of an acquisition function that balances exploration and exploitation when selecting additional samples in the design space. The results of this study, not shown here for the sake of brevity, indicated that the lower-confidence bound (LCB) acquisition function ensure convergence to the global maximum. Using the baseline design with the 75° spray targeting angle as the initial condition, the BOpt model suggests new design candidates in each design iteration that either show promise of maximizing the thermal efficiency at the C100 condition, or exist in regions of the design space that have not been explored and are characterized with merit value estimates with large uncertainty. At each iteration, a maximum of 8 new design candidates were generated using local penalization as a part of the batch optimization strategy in GPyOpt [30]. For each iteration, the design candidates that could not satisfy the compression ratio requirement of 19.2:1 were discarded. The optimization process was carried out until convergence in the thermal efficiency predictions was achieved, as defined by no change in the predicted merit value across five consecutive iterations. It is important to note that this convergence criteria does not guarantee convergence to the global maximum. However, careful selection of the acquisition function that balances exploration and exploitation and the use of batch optimization, or the evaluation of multiple design candidates per iteration, seeks to prevent premature convergence to a local maximum.

Figure 12 shows the evolution of the maximum thermal efficiency during BOpt analysis (red solid line). It can be observed that a candidate design was identified at the 5^{th} design iteration, or after a total of 40 CFD evaluations, that exceed the performance the single design determined from the DoE approach based on samples within the 11-D design space (1.45 percentage points), as well as the optimum design identified from the 165-point DoE analysis performed on 10-D design space with fixed spray targeting angle (1.88 percentage points). The optimization was performed for five additional iterations with no increase in the predicted merit value. The piston bowl visualized in Figure 13 achieved a thermal efficiency increase of 1.90 percentage points relative to the baseline design. It can be observed that the optimal design found by BOpt features a larger lip radius and a smaller lip radius of curvature with a flatter piston bowl rim compared to the baseline design.

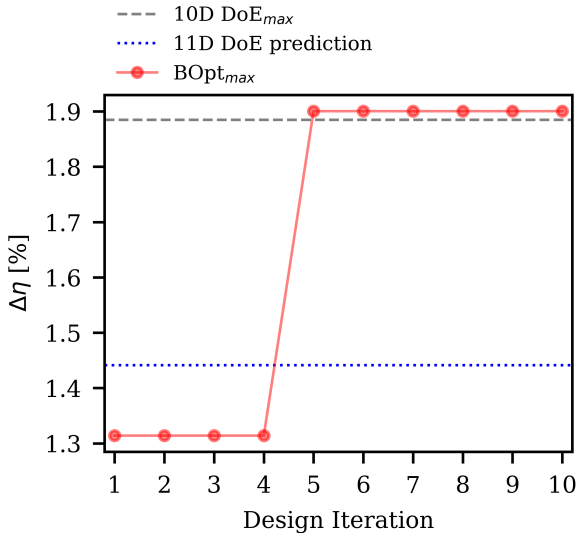

FIGURE 12: THE MAXIMUM INDICATED EFFICIENCY IMPROVEMENT OBTAINED WITH BAYESIAN OPTIMIZATION, COMPARED WITH THE MAXIMUM VALUES FROM THE 10-D and 11-D DOE ANALYSES.

6 CONCLUSIONS

Alcohol-fueled compression ignition (CI) engines are a promising solution for heavy-duty engine applications due to its fuel chemical characteristics. However, modifications to the existing CI engine configurations are required to utilize alcohol-based fuels, due to their low cetane number and high auto-ignition temperatures. This study builds on upon the previous work by authors, and investigates design optimization opportunities for alcohol-fueled CI engines used in heavy duty applications. Due to low soot and easy to perform aftertreatment NOx emissions, the optimization criteria for the alcohol-fueled

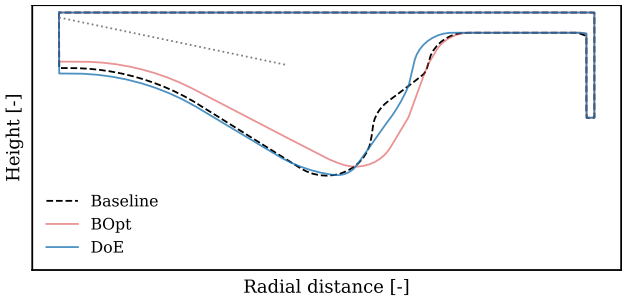

FIGURE 13: FINAL DESIGNS PROPOSED BY THE DOE AND THE BAYESIAN OPTIMIZATION. A LOWER-CONFIDENCE BOUND ACQUISITION FUNCTION WAS USED, BASED ON THE INITIAL TESTS PERFORMED ON A SIX-HUMP CAMEL TEST PROBLEM [29].

CI engine was identified as the indicated thermal efficiency. To identify piston bowl and spray targeting angle conditions optimal for alcohol-fueled CI engine combustion, a 3-D CFD framework coupled with a 1-D conjugate heat transfer (CHT) boundary modeling approach was developed and validated against experiments. In this work, a combined DoE and response surface methodology was employed as a baseline framework to identify optimal piston bowl-spray targeting angle configurations within a multi-dimensional design space that maximize the indicated thermal efficiency across a range of operating conditions. The computational expense of the design study motivated the exploration of a BOpt approach to identify high performing designs with lower computational expense. Based on the findings, the following conclusions are made:

1. A sector mesh engine CFD model with a 1-D CHT boundary condition was developed to represent the performance of a multi-cylinder engine using diesel and ethanol fuels across a range of operating conditions representing a drive cycle of interest. These simulations require ≈400 times less CPU-hours than their 3D open-cycle engine simulation counterparts, while providing a pressure trace profile with less than 1% deviation from fully open-cycle simulations. The sector mesh engine simulations agree with the experimentally measured peak pressure and indicated thermal efficiency within 0.1 MPa and 2.5 percentage points, respectively.
2. The 11-D DoE analysis investigating 165 designs revealed a candidate design that increases the ethanol-fueled CI thermal efficiency between 1.9 to 2.2 percentage points across four different operating conditions compared to the baseline piston bowl-spray targeting angle design. The proposed design features a smaller lip radius and a larger spray targeting angle relative to the baseline design.
3. The proposed candidate design results in the formation of a more homogeneous distribution of equivalence ratio and combustion temperature, and subsequently higher indicated thermal efficiency compared to the baseline design. All of these factors contribute to the decrease in exhaust temperatures and overall higher thermal efficiency in the optimal design across all operating conditions.
4. Bayesian optimization method was employed to find a candidate piston bowl design that uses the baseline spray targeting angle to avoid manufacturing a new injector. This approach revealed a candidate piston bowl design that provides a 1.9 percentage point increase in thermal efficiency, using the baseline spray targeting angle. The number of CFD simulations in this analysis required 65% less data samples relative to the 10-dimensional DoE analysis and avoided the computational cost of running a new DoE campaign.

The Bayesian optimization approach demonstrated in this work is a promising tool for guiding design improvements in CI engines operated with alternative fuels. In the future, the authors plan to extend this framework to investigate optimal combustion recipes for alcohol-fueled CI operating conditions (e.g., intake temperature, injection timing, injection pressure, injected fuel mass, swirl ratio).

ACKNOWLEDGMENT

The submitted manuscript has been created by UChicago Argonne, LLC, Operator of Argonne National Laboratory (Argonne). Argonne, a U.S. Department of Energy Office (DOE) of Science laboratory, is operated under Contract No. DE-AC02-06CH11357. The U.S. Government retains for itself, and others acting on its behalf, a paid-up nonexclusive, irrevocable worldwide license in said article to reproduce, prepare derivative works, distribute copies to the public, and perform publicly and display publicly, by or on behalf of the Government.

Argonne National Laboratory's work was supported through U.S. Department of Energy's Small Business Innovation Research (SBIR) program. The authors gratefully acknowledge the computing resources provided on Blues, a high-performance computing cluster operated by the Laboratory Computing Resource Center at Argonne National Laboratory, and Convergent Science Inc., for providing the CONVERGE CFD software licenses.

The authors would also like to thank Cummins Inc. for providing the mesh and CONVERGE setup, as well as Carsten Fuetterer and Mattia Brenner from Friendship Systems AG for their help in setting up CAESES for the engine design optimization study.

REFERENCES

[1] Global market insights, marine diesel engine market size by technology and application, industry analysis report for

2020 – 2026. https://www.gminsights.com/. 2019.
[2] Hua, Y., Liu, F., Wu, H., Lee, C.-F., and Li, Y., 2021. "Effects of alcohol addition to traditional fuels on soot formation: A review". *International Journal of Engine Research,* ***22***(5), pp. 1395–1420.
[3] Chase, S. A., Nevin, R. M., Winsor, R. E., and Baumgard, K. J., 2007. "Stoichiometric compression ignition (SCI) engine".
[4] Yates, A., Bell, A., and Swarts, A., 2010. "Insights relating to the autoignition characteristics of alcohol fuels". *Fuel,* ***89***(1), pp. 83–93.
[5] Natarajan, K., and Bhaskaran, K., 1981. An experimental and analytical investigation of high temperature ignition of ethanol. Tech. rep., Indian Inst. of Tech. Madras.
[6] Blumreiter, J., Johnson, B. H., Zhou, A., Magnotti, G. M., Longman, D., and Som, S. "Mixing-limited combustion of alcohol fuels in a diesel engine".
[7] Magnotti, G. M., Mohapatra, C. K., Mashayekh, A., Wijeyakulasuriya, S., Schanz, R., Blumreiter, J., Johnson, B. H., El-Hannouny, E. M., Longman, D. E., and Som, S., 2021. "Development of an efficient conjugate heat transfer modeling framework to optimize mixing-limited combustion of ethanol in a diesel engine". *Journal of Engineering for Gas Turbines and Power,* ***143***(9), 05.
[8] Yan, Z., Gainey, B., Gohn, J., Hariharan, D., Saputo, J., Schmidt, C., Caliari, F., Sampath, S., and Lawler, B., 2021. "A comprehensive experimental investigation of low-temperature combustion with thick thermal barrier coatings". *Energy,* ***222***, p. 119954.
[9] Pei, Y., Pal, P., Zhang, Y., Traver, M., Cleary, D., Futterer, C., Brenner, M., Probst, D., and Som, S., 2019. "Cfd-guided combustion system optimization of a gasoline range fuel in a heavy-duty compression ignition engine using automatic piston geometry generation and a supercomputer". *SAE Technical Papers*.
[10] Moiz, A. A., Pal, P., Probst, D., Pei, Y., Zhang, Y., Som, S., and Kodavasal, J., 2018. "A machine learning-genetic algorithm (ML-GA) approach for rapid optimization using high-performance computing". *SAE International Journal of Commercial Vehicles*, 4, pp. 291–306.
[11] Owoyele, O., Pal, P., Torreira, A. V., Probst, D., Shaxted, M., Wilde, M., and Senecal, P. K., 0. "Application of an automated machine learning-genetic algorithm (AutoML-GA) coupled with computational fluid dynamics simulations for rapid engine design optimization". *International Journal of Engine Research,* ***0***(0), p. 14680874211023466.
[12] Owoyele, O., and Pal, P., 2021. "A novel machine learning-based optimization algorithm (ActivO) for accelerating simulation-driven engine design". *Applied Energy,* ***285***, p. 116455.
[13] Badra, J. A., Khaled, F., Tang, M., Pei, Y., Kodavasal, J., Pal, P., Owoyele, O., Fuetterer, C., Mattia, B., and Aamir, F., 2021. "Engine combustion system optimization using computational fluid dynamics and machine learning: A methodological approach". *Journal of Energy Resources Technology, Transactions of the ASME,* ***143***, 2.
[14] Richards, K. J., Senecal, P. K., and Pomraning, E., 2021. Converge 3.0. Convergent Science, Madison, WI.
[15] Reitz, R., 1987. "Modeling atomization processes in high-pressure vaporizing sprays". *Atomisation Spray Technology,* ***3***, 01, pp. 309–337.
[16] Reitz, R. D., and Beale, J. C., 1999. "Modeling spray atomization with the kelvin-helmholtz/rayleigh-taylor hybrid model". *Atomization and Sprays*.
[17] Schmidt, D. P., and Rutland, C. J., 2000. "A new droplet collision algorithm". *Journal of Computational Physics,* ***164***, pp. 62–80.
[18] Frössling, N. Evaporation, heat transfer and velocity distribution in two-dimensional and rotationally symmetrical laminar boundary-layer flow. N.A.C.A. ADB1891. Tech. rep.
[19] Wang, H., Dempsey, A., Yao, M., Jia, M., and Reitz, R., 2014. "Kinetic and numerical study on the effects of ditert -butyl peroxide additive on the reactivity of methanol and ethanol". *Energy Fuels,* ***28***, 08, pp. 5480–5488.
[20] Jankovic, A., Chaudhary, G., and Goia, F., 2021. "Designing the design of experiments (doe) – an investigation on the influence of different factorial designs on the characterization of complex systems". *Energy and Buildings,* ***250***, p. 111298.
[21] CAESES Software. https://caeses.com. 2021.
[22] McKay, M. D., Beckman, R. J., and Conover, W. J., 1979. "A comparison of three methods for selecting values of input variables in the analysis of output from a computer code". *Technometrics,* ***21***(2), pp. 239–245.
[23] Deaconu, S., and Coleman, H. W., 2000. "Limitations of Statistical Design of Experiments Approaches in Engineering Testing ". *Journal of Fluids Engineering,* ***122***(2), 03, pp. 254–259.
[24] Dogan, G. L., Demir, S. O., Gutzler, R., Gruhn, H., Dayan, C. B., Sanli, U. T., Silber, C., Culha, U., Sitti, M., Tz, G. S., Grévent, C., and Keskinbora, K., 2021. "Bayesian machine learning for efficient minimization of defects in ald passivation layers". *ACS Applied Materials Interfaces*, 11, p. acsami.1c14586.
[25] Mondal, S., Magnotti, G. M., Lusch, B., Maulik, R., and Torelli, R., 2021. "Machine Learning-Enabled Prediction of Transient Injection Map In Automotive Injectors With Uncertainty Quantification". Vol. ASME 2021 Internal Combustion Engine Division Fall Technical Conference.
[26] Rasmussen, C., and Williams, C., 2005. *Gaussian Processes for Machine Learning*. Adaptive Computation and Machine Learning series. MIT Press.
[27] Garnett, R., 2015. Lecture notes in

bayesian methods in machine learning. https://www.cse.wustl.edu/~garnett/cse515t/spring_2015.
[28] GPyOpt: A Bayesian Optimization framework in Python. http://github.com/SheffieldML/GPyOpt. 2016.
[29] Molga, M., and Smutnicki, C., 2005. "Test Functions for Optimization Needs".
[30] González, J., Dai, Z., Hennig, P., and Lawrence, N. D., 2015. Batch bayesian optimization via local penalization.